Structure Control of π-Conjugated Polymers for Enhanced Solid-State Luminescence: Synthesis and Liquid Crystalline and Photophysical Properties of New Bulky Poly(*p*-phenylenevinylene)s and Oligo(phenylenevinylene)s Bearing Tricyclodecane Pendants

S. R. Amrutha and M. Jayakannan*

Polymer Research Group, Chemical Sciences & Technology Division, Regional Research Laboratory, Thiruvananthapuram 695019, Kerala, India

Received December 1, 2006; Revised Manuscript Received January 27, 2007

ABSTRACT: A series of novel highly luminescent bulky oligo(phenylenevinylene)s (MTCD−OPV, BTCD−OPV, and MEH−OPV), bulky π-conjugated poly(*p*-phenylenevinylene)s (MTCD−PPV, BTCD−PPV), and symmetrically or unsymmetrically substituted bulky random PPV copolymers (BTCD-*x* and MTCD-*x* series, where $x = 0-100$ mol %) bearing tricylodecane (TCD) pendants were synthesized to trace the factors which control the molecular aggregation of π-conjugated materials. The ^{1}H NMR signals of the OPVs were utilized to identify different types of repeating units in the copolymer backbone for determining their compositions. The thermal analysis revealed that all the polymers were highly amorphous, and the plots of T_g vs the composition of copolymers followed straight line Flory−Fox trend for a wider temperature ranging from 75 to 200 °C. The emission studies indicate that the copolymers with high rigidity (or high T_g) showed 4−5 times enhancement in photoluminescence (PL) intensity in the solid state and doubling of quantum yield in solution compared to MEH−PPV. The CPK space-filling model confirmed that bulky TCD substitution in the PPV induces strong steric hindrance and increases the intra- or interchain distances in the polymer backbone, which in turn control the π-stack-induced molecular aggregation for high PL intensity. The luminescence of oligo(phenylenevinylene)s (OPVs) was unique to their pendant groups, and their absolute solid-state quantum efficiency determined by diffuse reflectance techniques revealed that TCD-substituted molecules MTCD−OPV and BTCD−OPV showed enhancement in the quantum efficiency (82 and 64%, respectively) compared to the MEH−OPV (27%). The thermal analysis and PLM observation of the OPV molecules indicate that while cooling from melt the TCD unit in MTCD−OPV hinders the packing of the molecules and forces the entire matrix to trap into amorphous glassy domain. The glassy nature of the molecule contributes to the 82% quantum yield of MTCD−OPV, which is the first OPV in the literature with more than 80% solid-state luminescent quantum yield. The symmetrical substitution enhances lateral packing of molecules in BTCD−OPV, and it was found as a thermotropic nematic liquid crystalline material with 64% quantum yield. In a nutshell, here for the first time, we have successfully demonstrated that the chemical structure of the bulky π-conjugated materials plays a major role in the manipulation of solid-state luminescent intensity, quantum yield, liquid crystalline and amorphous glassy nature of PPVs, and its triad oligomers.

Introduction

Luminescent conducting polymeric materials have attracted wide interest followed by the discovery of light-emitting phenomena by the Cambridge group.[1,2] π-Conjugated polymers based optoelectronic devices are proving to be very promising due to their low cost, multicolored and large area flat panel display, easy processing techniques, feasibility of designing various molecular structures, and mechanical, thermal, and environmental stability.[3−5] Though the polymeric emitters have many advantages, the reality of attaining high efficient devices are still premature because they need additional features like high quantum efficiency, low operating voltage, high pure sample, long lifetime, solubility of high molecular weight fractions, high photoluminescence (PL) and electroluminescence (EL) efficiency, etc.[6] The basic requirement for efficient polymeric emitter is that high efficiencies of formation of excimers upon shining light and subsequent high radiative emission.[7] Almost all the polymeric emitters do not have problem in the formation of excimers, however, many of them fail as highly luminescence emitters. It is generally believed that the intra- and intermolecular interactions between the conjugated polymers form weakly emissive species, and the excitation energy dissipated via nonradiative deactivation.[8] It is understood that the reduction in quantum yield is not due to the reduction in excited-state lifetime, and it is mainly due to the formation of nonemissive interchain species like π-induced molecular aggregation.[9] Even though the detailed identity of the interchain species is still under debate, a generally accepted understanding is that these aggregates rapidly quench the luminescent efficiency of the materials.[10−13] Now it has been recognized that the control of π-stack-induced molecular aggregation in the polymer chain is an important task in the development of highly emissive conjugated polymers and also making the ideal polymer luminescent optoelectronic devices in reality. Various chain separation techniques have been attempted to reduce the chain aggregation, among them thermal annealing of conjugated polymers above the glass transition temperature,[14] introduction of *cis*-vinylene linkages,[15−20] synthesis of block copolymers,[21−24] and adding bulky side groups[25−29] for interchain separation are worth mentioning. The thermal annealing approach was successful to some extent, but it induces unwanted chain scissions and interruption of conjugation length.[14] The meta linkages allow the polymers to bend and

* Corresponding author: e-mail jayakannan18@yahoo.co.in, Fax 0091-471-2491712.

10.1021/ma062764q CCC: $37.00
Published on Web 03/06/2007

twist effectively and control the chain packing in the solid state; however, the HOMO−LUMO energies of the confined structures are different from the parent polymer, which often causes difficulty in choosing the work function of electrodes and also alters the color of emission.[15,16] The separation of interchain distances using suitable bulky anchoring groups is attractive because the aggregation can be controlled without altering the electronic properties of the parent polymer. Poly(2-methoxy-5-(2-ethylhexyloxy)-1,4-phenylenevinylene) (MEH−PPV) is one of the well-studied polymeric emitters because the rigid PPV backbone combined with alkoxy side groups provides necessary conformational degrees of freedom for higher solubility and processability. Attempts have been reported for bulky PPVs using alkoxy units of cyclohexyl,[30−32] adamantane[33,34] and cholestanyl rings,[35,36] aryloxy of phenyl,[37] biphenyl,[38] and naphthyl,[39] and inorganic pendants like silyl[40] and silsesquioxane[41,42] in PPV to control the molecular aggregation in the solid state. The advantages of the bulky anchoring groups are that they increase the glass transition temperature (T_g) of the PPV, and high T_g is an important parameter for long operating lifetime of devices.[43] However, some of the most efficient bulky PPVs were reported insoluble in common solvents, which limit their processability, complete structural characterization, molecular weight determination, etc.[33,35] Chou et al. have attempted to increase the solubility via the copolymerization approach in the rigid silsesquioxane-substituted PPV; however, the studies were restricted to 10 mol % due to poor solubility, and the effect of bulky pendants in a large window of composition is so far not known.[41] Utilizing structurally similar bulky model compounds to address the solid-state luminescence behavior of the bulky PPV is an attractive approach, which is also not explored. There are isolated reports for sterically hindered highly luminescent oligo(phenylenevinylene) materials; however, no effort has been taken to study the effect of same bulky pendants in high molecular weight PPV polymers.[44−47] Therefore, the overall ramifications of important development in improving the luminescence intensity and tracing the factors behind the molecular aggregation in the highly luminescent bulky PPVs for optoelectronic applications are challenging problems to be addressed.

Recently, we have reported new soluble, processable, and highly luminescence tricyclodecane (TCD)-substituted PPVs, and the role of the bulky TCD unit was investigated on the photoluminescence properties of PPV in both solution and solid state.[48] The preliminary investigation revealed that π-stack induced aggregates in PPV was controlled successfully by the TCD units and a large enhancement of solid-state photoluminescence was observed. TCD is a very attractive bulky anchoring group for π-conjugated polymers because of its tricyclic rigid bulky structure; also, it is sluggish to crystallize, has low cost, and has commercial availability compared to many anchoring units earlier reported for bulky PPVs. In the present report, we have utilized the advantages of TCD bulky unit and addressed few important fundamental questions in bulky PPVs, and the novelties are as follows: (i) Two series of copolymers of symmetrically and unsymmetrically substituted tricyclodecane PPV's with MEH−PPV were prepared (MTCD-*x* and BTCD-*x* series; see Scheme 1) and the copolymerization effect on the photophysical and thermal properties were investigated, for the first time, in the entire composition range from 0 to 100%. (ii) In order to trace the origin of the enhancement of solid-state luminescence in bulky PPVs, we have also synthesized three oligo(phenylenevinylene)s (OPVs)—1-(methoxy)-4-(2-ethylhexyloxy)-2,5-distryrylbenzene (MEH−OPV), 1-(methoxy)-4-(1,8-tricyclodecanemethyleneoxy)-2,5-distryrylbenzene (MTCD−OPV), and 1,4-bis(1,8-tricyclodecanemethyleneoxy)-2,5-distryrylbenzene (BTCD−OPV)—which are structurally similar to their bulky PPVs. (iii) Using NMR features of the oligomers, the copolymer composition was determined, which is very crucial parameter for correlating the photophysical properties of the copolymers to their structure. (iv) We have proven that the rigid bulky PPV polymers follow the Flory−Fox trend for the glass transition of copolymers and highly rigid structures showed photoluminescence enhancement 4−5 times higher than that of MEH−PPV. (v) The absolute solid-state quantum yields of the OPVs were determined by the diffuse reflectance method, and the values suggest that the bulky substitution increases the solid-state quantum efficiency of the MEH−OPV from 27% to 82%, which directly give evidence for highly luminescence behavior of the bulky π-conjugated polymers. (vi) Depending upon the substitution in the backbone, the bulky OPV pack differently in the solid state: the MTCD−OPV was obtained as highly amorphous glass with more than 82% solid-state quantum efficiency, whereas the BTCD−OPV molecules showed thread-like nematic liquid crystalline phases with 64% solid-state quantum efficiency. In a nutshell, here we have successfully demonstrated that the role of bulky substituents is a crucial factor to achieve high emissive oligo(phenylenevinylene)s and PPVs. We have carried out a detailed photophysical and thermal analysis to trace the factors behind the π-stack-induced aggregation in the polymer chains to explore the development of futuristic highly luminescent π-conjugated materials.

Experimental Methods

Materials. *p*-Toluenesulfonyl chloride, 4-methoxyphenol, hydroquinone, 2-ethylhexyl bromide, potassium *tert*-butoxide, Rhodamine-6G, and quinine sulfate were purchased from Aldrich Chemicals. Sodium salicylate (99.5%) was purchased from Merck Chemicals. HBr in glacial acetic acid, paraformaldehyde, and all other reagents/solvents were purchased locally and purified by following the standard procedures. 1,8-Tricyclodecanemethanol (TCD) was donated by Celanese Chemicals & Co. and used without further purification. 1-Methoxy-4-(2-ethylhexyloxy)benzene, 1-methoxy-4-(1,8-tricylodecanemethyleneoxybenzene), 1,4-bis(1,8-tricyclodecanemethyleneoxy)benzene, 1,4-bis(bromomethyl)-2-methyloxy-5-(2-ethylhexyloxy)benzene (**1**), 1,4-bis(bromomethyl)-2-methyloxy-5-(1,8-tricyclodecanemethyleneoxy)benzene (**2**), and 1,4-bis(bromomethyl)-2,5-di(1,8-tricyclodecanemethyleneoxy)benzene (**3**) were synthesized as reported earlier.[48]

General Procedures. ^{1}H and ^{13}C NMR spectra of the compounds and polymers were recorded using a 300 MHz Bruker NMR spectrophotometer in $CDCl_3$, containing a small amount of TMS as internal standard. Infrared spectra of the samples were recorded with a Pekin Elmer Fourier transform infrared (FTIR) spectrophotometer in the solid state. The purity of the monomers, model compounds, etc., was determined by JEOL JSM600 fast atom bombardment (FAB) high-resolution mass spectrometry. The compound was dissolved in $CHCl_3$ and suspended in 3-nitrobenzyl alcohol as a matrix for FAB−mass measurements. Elemental analyses of the model compounds and polymers were carried out using an Elementar Vario EL-III CHN analyzer. The thermal stability of the polymers was determined using a TGA-50 Shimadzu thermogravimetric analyzer at a heating rate of 10 °C/min in nitrogen atmosphere. Thermal analyses of the polymers were performed with a Perkin-Elmer Pyris-6 differential scanning calorimetry (DSC) instrument under nitrogen, and the instrument was calibrated with indium, tin, and lead standards. All samples were first heated to melt at 280 °C prior to recording their thermograms to remove their previous thermal history and recorded using a heating/cooling rate of 10 °C/min under the purge of dry nitrogen. The liquid crystalline properties of the polymers were investigated

using a Nikon HFX 35 A Optiphot 2-Pol polarized light optical microscope equipped with a Linkam THMS 600 heating and freezing stage connected to a Linkam TMS 93 temperature programmer. The molecular weights of the polymers were determined by gel permeation chromatography (GPC) in tetrahydrofuran (THF) using polystyrene as standards. The flow rate of THF was maintained as 1 mL/min. The polymer solution was prepared by dissolving 3 mg of the sample in 1 mL of THF, filtered, and injected for recording the GPC chromatograms. The chromatograms were recorded using a Waters 510 pump, a Waters 2487 UV−vis detector, and a Waters 410 differential RI detector. Three mixed styra-gel columns in series HT 6E, HR 5E, and HR 4E were employed for the separation. The absorption and emission studies were done by a Perkin-Elmer Lambda 35 UV−vis spectrophotometer and Spex-Fluorolog DM3000F spectrofluorometer with a double-grating 0.22 m Spex 1680 monochromator and a 450 W Xe lamp as the excitation source using the front-face mode. The solution spectra were recorded in chloroform, and for the solid-state spectra, polymers thin films (10−100 μM) were prepared by spin-casting chloroform solution on glass substrates. The solution emission quantum efficiencies of the polymers were determined by excitation at 480 nm in chloroform. Rhodamine 6G in water (ϕ = 0.95) was employed as standard, and the concentrations of polymer solution and standard were adjusted in such a way to obtain the absorbance equal to 0.1 at 480 nm.[48,49] Similarly the quantum yields of the OPVs were determined using quinine sulfate in 0.1 M H_2SO_4 (ϕ = 0.546) instead of Rhodamine 6G. The absolute solid-state emission quantum yields of the OPVs were measured at room temperature using the diffuse reflectance technique described by Bril et al.[50] using sodium salicylate as standard.[51−53]

1-(Methoxy)-4-(1,8-tricyclodecanemethyleneoxy)-2,5-distryrylbenzene (MTCD−OPV). 1,4-Bis(bromomethyl)-2-methyloxy-5-(1,8-tricyclodecanemethyleneoxy)benzene (**2**) (2.00 g, 4.4 mmol) and triethyl phosphite (1.46 g, 8.8 mmol) were heated to 140−150 °C for 12 h under a nitrogen atmosphere. Excess triethyl phosphite was removed by vacuum distillation, and the resultant ylide 1-(methoxy)-4-(tricyclodecanemethyleneoxy)-2,5-xylenetetraethyldiphosphonate (**5**) was obtained as a thick oil. ^{1}H NMR ($CDCl_3$) δ: 6.89 ppm (d,2H, Ar−H), 4.03 ppm(m, 8H, −PO−OCH_2), 3.76 ppm (s, 3H, Ar−OCH_3), 3.60 ppm (m, 2H, Ar−OCH_2), 3.20 ppm (m, 4H, Ar−CH_2P), 1.49−0.99 ppm (m, 27H, aliphatic). FT-IR (cm^{-1}): 3444, 2948, 2868, 2401, 1720, 1649, 1511, 1470, 1410, 1393, 1369, 1308, 1248, 1216, 1160, 1095, 1027, 963, 889, 524 cm^{-1}. To the crude ylide (2.30 g, 4.0 mmol) in 50 mL of dry THF, benzaldehyde (1.06 g, 10.0 mmol) and potassium *tert*-butoxide in (10 mL, 1 M THF) were added, and the contents were stirred under nitrogen for 12 h at 30 °C. It was poured into methanol, and the yellow solid was filtered and purified by passing through a silica gel column using ethyl acetate and hexane (1:20 v/v) as eluent. Yield = 40%; mp = 175−176 °C. ^{1}H NMR ($CDCl_3$) δ: 7.56−7.09 ppm (m, 16H, Ar−H and vinylic H), 3.91 ppm (s, 3H, Ar−OCH_3), 3.87−3.77 ppm (m, 2H, Ar−OCH_2), 2.31−0.96 ppm (m, 15H, cyclic-H). ^{13}C NMR ($CDCl_3$) δ: 151.5, 138.0,129.1, 127.4, 126.9, 123.3, 111.0, 109.6 (**Ar**−C), 73.8 (**Ar**−OCH_3), 56.4 (**Ar**−OCH_2), 45.7, 45.3, 44.0, 41.3, 40.3, 29.7, 29.1, 28.0, 27.0, and 26.5 ppm (**cyclic-C**). FT-IR (cm^{-1}): 3357, 2939, 2868, 1733, 1593, 1495, 1456, 1410, 1338, 1253, 1201, 1108, 1036, 963 (HC═CH, trans), 875 (HC═CH, cis), 861, 839, 751 cm^{-1}. HRMS (MW: 476.7): m/z = 476.4 (M^+). Anal. Calcd for $C_{34}H_{36}O_2$: C, 85.67; H, 7.61. Found: C, 85.51; H, 7.97.

A similar procedure was adopted for the synthesis of model compounds MEH−OPV and BTCD−OPV. (Structural characterization and elemental analysis data are available as Supporting Information.)

Synthesis of Poly(*p*-phenyelenevinylene)s. A typical polymerization procedure is described for poly[2-methoxy-5-(tricyclodecanemethyleoxy)-1,4-phenyelenevinylene)] (MTCD−PPV). **2** (0.28 g, 6.0 mmol) was dissolved in dry THF (50 mL), and potassium *tert*-butoxide (6 mL, 1 M THF) was added to the solution and stirred well under a nitrogen atmosphere for 24 h at 30 °C. The red precipitate was poured in to methanol, filtered, and washed successively with methanol and acetone. The red precipitate was further purified by Soxhlet extraction using methanol, hexane, and acetone. It was dried in vacuum oven at 40 °C for 5 h prior to further analysis. Yield = 0.11 g (64%). ^{1}H NMR ($CDCl_3$) δ: 7.63 ppm (b, 2H, **Ar**−H), 7.19 ppm (s, 2H, **CH═CH**), 3.95 ppm (s, 3H, −**OCH_3**), 3.83−3.49 ppm (b, 2H, −**OCH_2**), 2.45−0.90 ppm (m, 15H, **cyclic**). FT-IR (KBr, cm^{-1}): 3264, 2949,2862, 1608, 1502, 1409, 1351, 1314, 1252, 1201, 1040, 968 (HC═CH, trans), 861, 780, 698, and 619 cm^{-1}. Anal. Calcd for $[C_{20}H_{24}O_2]_n$: C, 81.04; H, 8.16. Found: C, 80.83; H, 8.38.

Similarly, the monomers **1** and **3** were polymerized using potassium *tert*-butoxide to obtain the polymers poly(2-methoxy-5-(2-ethylhexyloxy)-1,4-phenylenevinylene) (MEH−PPV) and poly[bis-2,5(1,8-tricyclodecanemethyleneoxy-)1,4-phenylenevinylene] (BTCD−PPV), respectively (for NMR, FT-IR, and elemental analysis data, see Supporting Information).

Results and Discussion

The syntheses of novel bulky π-conjugated polymers and oligomers are shown in Scheme 1. Poly[2-methoxy-5-(1,8-tricyclodecanemethyleneoxy)-1,4-phenylenevinylene] **(**MTCD−PPV), poly[bis-2,5-(1,8-tricyclodecanemethyleneoxy)-1,4-phenylenevinylene] **(**BTCD−PPV), and poly[2-methoxy-5-(2-ethylhexyloxy)-1,4-phenylenevinylene] **(**MEH−PPV) were prepared by polymerizing their respective monomers **2, 3**, and **1** in the presence of potassium *tert*-butoxide as base in dry tetrahydrofuran, respectively. Two series of bulky copolymers MTCD-*x* and BTCD-*x* were synthesized by varying the mole ratios of the monomers **2** or **3** with **1** in the feed (5, 10, 15, 20, 35, 50, 63, 75, and 90 mol %) under the identical experimental conditions employed for homopolymers. Three oligo(phenylenevinylene)s (OPVs)—1-(methoxy)-4-(2-ethylhexyloxy)-2,5-distryrylbenzene **(**MEH−OPV), 1-(methoxy)-4-(1,8-tricyclodecanemethyleneoxy)-2,5-distryrylbenzene **(**MTCD−OPV), and 1,4-bis(1,8-tricyclodecanemethyleneoxy)-2,5-distryrylbenzene **(**BTCD−OPV) were also synthesized by reacting the bis-ylides of **1**, **2**, and **3** with benzaldehyde under Wittig reaction conditions. The structures of the polymers and OPVs were confirmed by ^{1}H NMR and FT-IR. One of the limitations, in general, noticed in the earlier reports based on bulky-PPVs, was the poor structural characterization of the polymers by NMR due to the difficulty in the identification of protons corresponding to different subunits in the polymer backbone.[33,35] Interestingly, in the present investigation, the alkoxy protons of the OPVs showed a significant difference in their ^{1}H NMR spectra for structural difference in their repeating units, which was utilized directly to quantify the compositions of the MTCD-*x* and BTCD-*x* copolymers. The ^{1}H NMR spectra of MTCD-*x* copolymer**,** BTCD-*x* copolymer, and three OPVs are shown in Figure 1. The various types of alkoxy protons are assigned by letters in Figure 1. In Figure 1a,b, the Ar−OC**H_2**−TCD protons (type c) in BTCD−OPV and MTCD−OPV appeared as a multiplet at 3.80−3.67 ppm. The Ar−OC**H_3** (type a) is magnetically different from Ar−OC**H_2**−TCD in MTCD−OPV and appeared as a singlet at 3.90 ppm. The Ar−OC**H_2**−EH (type b) and Ar−OC**H_3** (type a) in MEH−OPV (in Figure 1c) appeared as a closely packed doublet + singlet at 3.90−3.85 ppm. The ^{1}H NMR spectra of OPVs clearly indicate that the chemical shift values of the Ar−OC**H_2**− protons are highly sensitive to their structural difference, and therefore, the two types of repeating units in the copolymers can be distinguishable by these structural variation. In BTCD-*x* copolymers (Figure 1d), the alkoxy protons in the MEH−PPV repeating unit (a + b) appeared as a broad peak, which is well separated from the alkoxy protons corresponding to the Ar−OC**H_2**TCD of the BTCD repeating unit (proton c). Similarly in the MTCD

Scheme 1. Synthesis of New Bulky PPVs and Oligo(phenylenevinylene)s

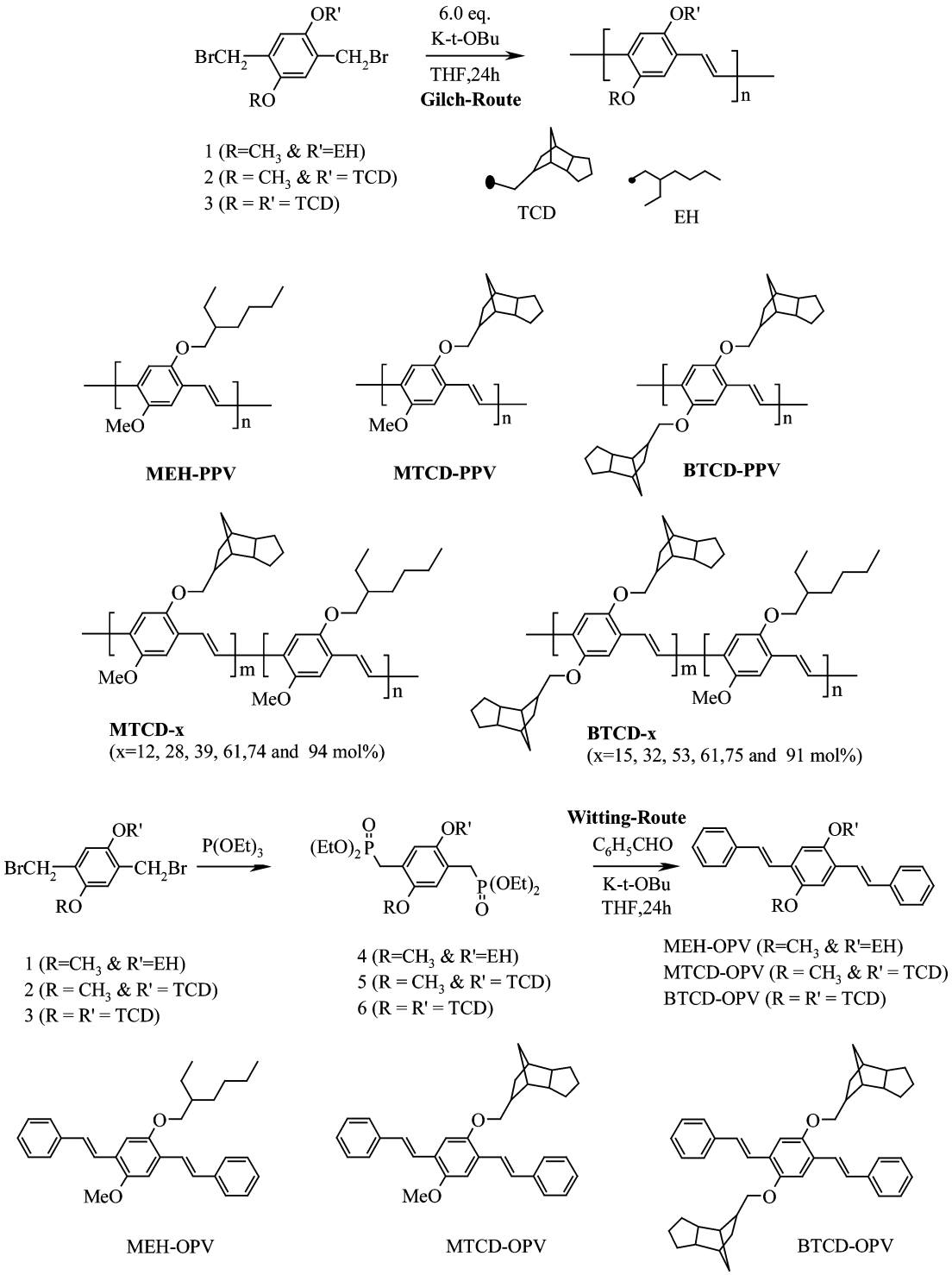

copolymers also the MEH−PPV protons (a + b) were clearly separated from the MTCD unit (a + c) protons. Therefore, the comparison of the intensities of these characteristic peaks gives the actual incorporation of MTCD or BTCD units in the MEH−PPV copolymers. The plots of the composition of the TCD unit in the copolymer vs feed (see Supporting Information) are shown as a straight line, which suggests that the copolymers follow a linear trend irrespective of their feed ratio. For less than 35% of MTCD and BTCD monomers in the feed, the alkoxy protons were not well-resolved, and therefore, their actual incorporation in copolymers was obtained theoretically by extra-plotting their plots (see Table 1). The copolymers are denoted as MTCD-*x* and BTCD-*x*, where *x* represents the actual incorporation of the bulky units in the MEH−PPV backbone. Infrared spectra (FT-IR) of all the polymers and model compounds (OPVs) were recorded in KBr pellets to identify the structure of the double bonds (cis and trans of vinylene double bonds) in the phenylenevinylene backbone (spectra are given in the Supporting Information). The FT-IR spectra of OPVs showed characteristic absorption bands at 2960, 2922 cm^{-1} (C−H stretching of the aliphatic units), 1600, 1501, 1458 cm^{-1} (C−H, aromatic ring), 1252, 1201 (C−O ether linkage), 965 cm^{-1} (trans HC═CH), and 875 cm^{-1} (cis HC═CH) vinylene C−H out-of-plane bending, and the values match those reported in the literature.[37a,g,54] The IR spectra of the polymers are almost identical to that of the OPVs, except the disappearance of the absorption

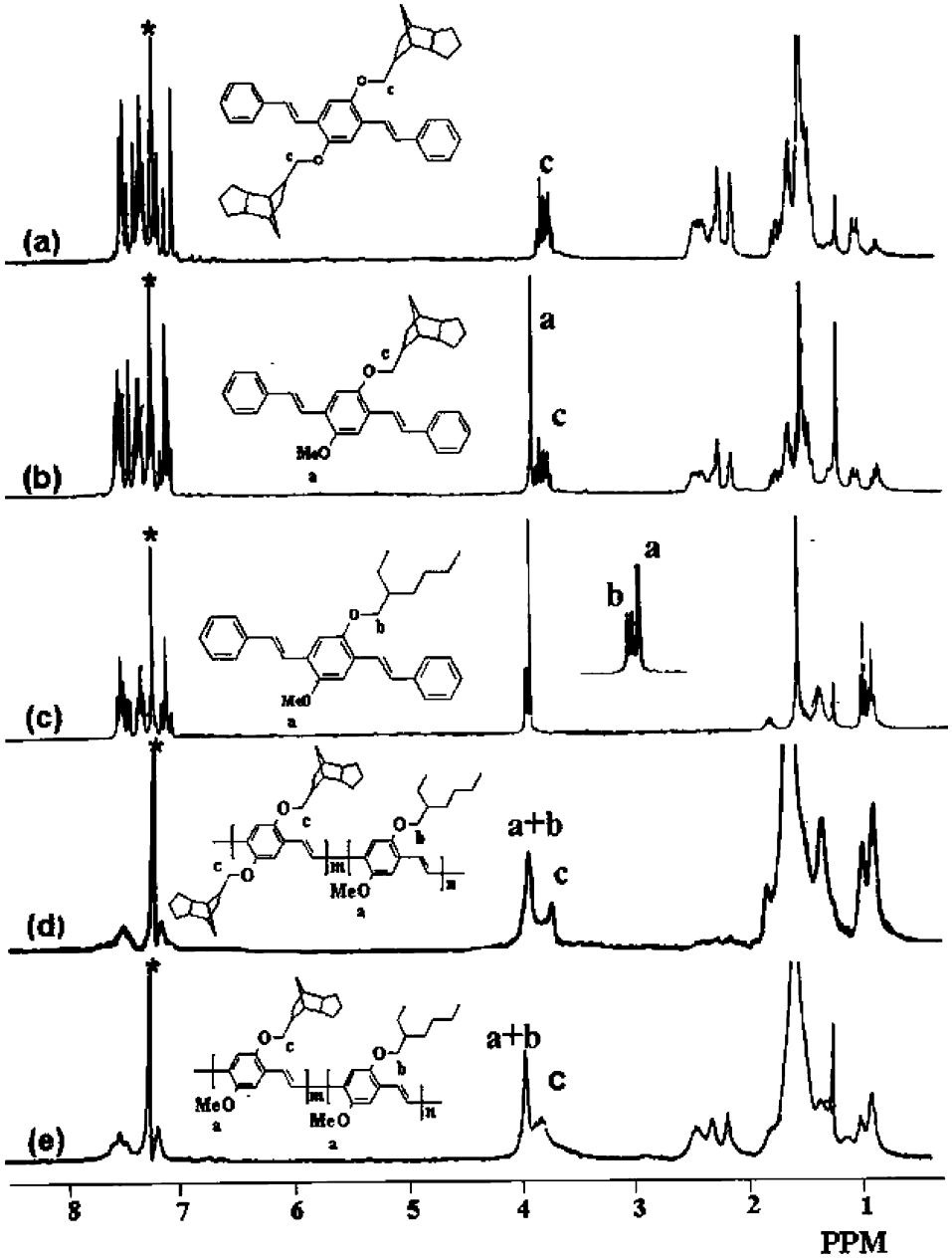

Figure 1. ^{1}H NMR spectra of BTCD−OPV (a), MTCD−OPV (b), MEH−OPV (c), BTCD-*x* (d), and MTCD-*x* (e) in $CDCl_3$. The peaks indicated by asterisk are corresponding to $CHCl_3$ in $CDCl_3$.

band for the *cis*-vinylene (at 875 cm^{-1}). It revealed that the polymers (homo- and copolymers) produced by the Gilch route have a more regular configuration and exist in the *trans*-vinylene HC═CH double bonds compared to that of the OPV oligomers which were synthesized through the Wittig reaction. Recently, Lee et al. reported a similar observation in their phenyl-substituted PPVs that the polymers produced via the Gilch route were found to have more *trans*-vinylene double bonds compared to the Wittig reaction.[37g] In the present investigation, irrespective of the structural differences in the pendant units (EH, mono-TCD, or bis-TCD), the Gilch route predominantly produced *trans*-vinylene double bonds in both homo- and copolymers (see FT-IR spectra in Supporting Information). The number- and weight-average molecular weights (M_n and M_w), polydispersities, and number-average degree of polymerization (*n*) of the polymers are summarized in Table 1. The molecular weights of the MEH−PPV are very high and comparable to the reported values,[14,15,55] which confirmed that the experimental conditions adopted for the synthesis is adequate enough for producing high molecular weight polymers by the Gilch route. MTCD−PPV is partially soluble in THF whereas the BTCD−PPV is insoluble in THF, and its molecular weight could not be determined. The MTCD-*x* copolymers were freely soluble up to 75% incorporation, whereas the BTCD-*x* copolymers were less soluble (up to 63%) compared to that of their mono-TCD counterparts. Therefore, only the soluble fractions of MTCD-94, MTCD−PPV, BTCD-61, and BTCD-91 were used for molecular weight determination. It suggests that the higher incorporation of bulky TCD groups decreases the solubility of the PPV, similar to that of other bulky derivatives such as cholestanyl,[35,36] adamantyl,[33−34] and silsesquioxane.[41] However, the numbers of repeating units in these soluble fractions of polymers are found in the range 11−32, which is sufficient enough to compare their structure−property relationships.

The absorbance spectra of the polymers were measured in chloroform, and they are given in Figure 2. The spectra of MTCD−PPV and BTCD−PPV were blue-shifted by 7 and 42 nm, respectively, compared to that of MEH−PPV, which

Table 1. Composition and Molecular Weights of the Bulky PPV Polymers

sample	TCD monomer in feed (mol %)	TCD amount in copolymers (mol %)[a]	M_p[b]	M_n[b]	M_w[b]	M_w/M_n[b]	n[e]
MEH−PPV	0	0	52 000	20 300	70 100	3.5	78
MTCD-12	10	11.8	70 800	22 400	96 100	4.3	76
MTCD-28	25	27.6	136 400	37 600	144 200	3.8	127
MTCD-39	35	39.0	127 200	47 900	14 100	2.9	162
MTCD-61	50	61.0	132 100	39 800	139 300	3.5	134
MTCD-74	75	74.0	40 300	17 200	443 900	2.6	58
MTCD-94[c]	90	93.8	29 800	9 600	31 000	3.2	32
MTCD−PPV[c]	100	100	5 900	5 400	12 500	2.3	18
BTCD-15	10	14.7	145 700	46 000	260 100	5.6	107
BTCD-32	20	31.7	47 000	25 500	71 300	2.8	59
BTCD-53	35	53.2	107 500	23 800	110 600	4.6	55
BTCD-61	50	60.8	19 300	9 300	23 900	2.6	22
BTCD-75[c]	63	75.0	9 700	6 100	16 900	2.7	14
BTCD-91[c]	75	90.8	4 100	4 800	11 700	2.5	11
BTCD−PPV	100	100	*d*				

[a] Determined by ^{1}H NMR spectroscopy. [b] Molecular weights are determined by gel permeation chromatography in THF at 30 °C using polystyrene standards for calibration. [c] Molecular weights determined for soluble fractions in THF only. [d] Insoluble in THF for molecular weight determination. [e] Calculated number-average degree of polymerization.

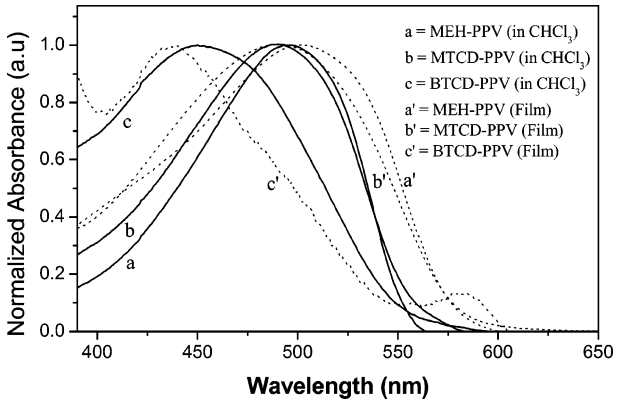

Figure 2. Absorbance spectra of the bulky PPVs in the solution and solid state.

indicates that the bulky TCD substitution strongly induce steric hindrance in the PPV backbone and disturbs the planarity of the polymer chain. The solid-state absorption spectra of polymer film are also shown in Figure 2. In general, the solid-state absorbance spectra of π-conjugated polymers were expected to show a red shift compared to their solution spectra because of strong $\pi-\pi$ overlap among the intra- or interpolymer chains in the solid state. As expected, the absorbance spectra of MEH−PPV is red-shifted by 7 nm in the film compared to its solution. The BTCD−PPV showed an opposite trend, and the absorbance spectrum is blue-shifted by 21 and 70 nm compared to its solution spectrum and that of MEH−PPV in film, respectively. The absorbance spectra of MTCD−PPV were 12 nm blue-shifted compared to MEH−PPV. It indicates that the mono-TCD substitution in the PPV backbone slightly affects the planarity of the polymer chains compared to its symmetrically substituted bis-TCD units. It is also important to note that the absorbance spectrum of BTCD−PPV has a shoulder at 580 nm, which corresponds to the lateral packing of symmetric structure. A similar trend of lateral packing of PPV chains is commonly noticed in symmetric substituted PPVs based on cholestanyl and adamantyl anchoring group.[6,34,35] The absorbance properties of the two series of copolymers MTCD-*x* and BTCD-*x* are in the range between their homopolymers (see Table 2).

The emission properties of the polymers were carried out in solution as well as in films by exciting at the absorbance maxima. The emission spectra of the homo- and copolymers showed almost similar behavior in chloroform, and there is no significant difference in their spectral features (see Supporting Information). The solid-state emission spectra (in film) of the polymers are shown in Figure 3, and their data are summarized in Table 2. The emission maxima of all the polymers were appeared almost in the same range irrespective of the difference in their solid-state absorbance spectra. In order to understand the nature of emissive species, the excitation spectra were recorded (see Supporting Information). The excitation spectra of all the polymers were almost identical, which confirms that though there is a large difference in the absorbance maxima between BTCD−PPV and other polymers (50−100 nm), the emissive species at the excited state are almost identical. The most significant observation in the emission studies is that the photoluminescence (PL) intensity of BTCD−PPV and MTCD−PPV is enhanced more than 4−5 times compared to that of MEH−PPV. The PL spectra of the copolymers showed an interesting observation, and their PL intensities are highly dependent on the composition of the copolymers (see Table 2). For instance, the PL intensity of the BTCD-75 is 3−4 times higher than that of the BTCD-32. Since the excitation spectra of the polymers are very broad from 420 to 550 nm (see Supporting Information), it is very important to investigate the variation in the PL intensity for different excitation energy (or wavelength). The emission spectra of the MEH−PPV and BTCD-75 were recorded using various excitation energies in the region of 400−550 nm, and the results indicate that the PL intensities of the polymers are almost the same for the various excitation energies (see inset in Figure 3). It confirms that the large enhancement in the PL intensity in the TCD-substituted polymers arose from their polymer backbone, and the chemical structure of the π-conjugated polymers plays a major role in the luminescent properties of the polymers. The quantum yields of the polymers in solution were determined using Rhodamime-6G as standard following the equation

$$\phi_s = \phi_r(F_sA_r/F_rA_s)(n_r/n_s)^2$$

where ϕ is the fluorescent quantum yield, F is the area of the emission, n is the refractive index of the solvent, and A is the absorbance of the solution at the exciting wavelength.[49] The subscripts r and s denote the reference and sample, respectively. The quantum yield of the MEH−PPV is calculated as 0.16, which is in accordance with earlier reports.[15,48] The quantum yields of the MTCD−PPV and BTCD−PPV (see Table 2) are almost twice compared to MEH−PPV, which indicates that the bulky substitution increase the quantum yield of the PPV backbone. The solid-state PL intensity of the copolymers and

Table 2. Photophysical and Thermal Properties of the Bulky PPV Polymers

	in $CHCl_3$			in film				
sample	λ_{max}(abs) (nm)	λ_{max}(em)[a] (nm)	ϕ_{FL}[b]	λ_{max}(abs) (nm)	λ_{max}(em)[c] (nm)	PL int ($\times 10^4$)	T_D[d] (°C)	T_g[e] (°C)
MEH−PPV	496	558	0.16	503	577	3.1	322	78
MTCD-12	495	555	0.20	503	587	5.9	322	79
MTCD-28	495	556	0.19	502	584	8.6	334	96
MTCD-39	494	556	0.20	505	582	6.7	349	105
MTCD-61	498	555	0.21	506	584	8.1	350	122
MTCD-74	494	555	0.21	508	581	21.4	320	140
MTCD-94	492	555	0.21	506	584	20..3	306	154
MTCD−PPV	489	559	0.29	491	582	25.2	302	174
BTCD-15	497	560	0.16	504	585	5.3	284	95
BTCD-32	495	559	0.16	501	573	4.5	360	103
BTCD-53	484	562	0.24	485	569	20.7	287	129
BTCD-61	493	560	0.25	506	587	17.2	303	143
BTCD-75	491	561	0.27	496	593	23.2	290	
BTCD-91	495	561	0.26	504	575	17.1	288	
BTCD−PPV	454	548	0.26	433	593	22.5	290	

[a] Absorption and emission studies were done in chloroform, and the excitation wavelength used is 480 nm for all the polymers. [b] Calculated using Rhodamine 6G as standard and excited at 480 nm; the absorbance of solutions was maintained as 0.1 at 480 nm. [c] Excitation wavelength is the absorbance maximum. [d] Decomposition temperature at 10% weight loss. [e] Glass transition temperature was obtained from DSC analysis at 10 °C/min heating rate.

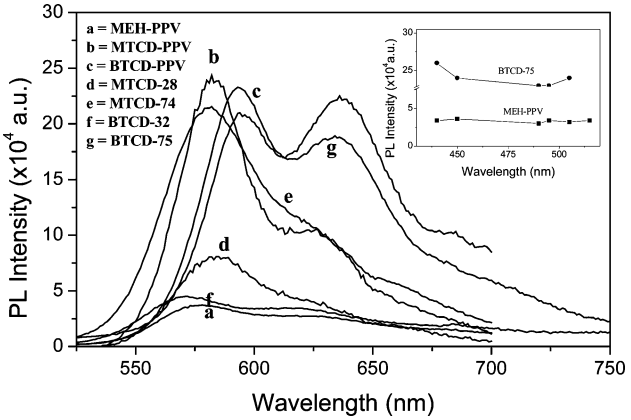

Figure 3. Solid-state emission spectra of the bulky PPVs. The excitation wavelength vs PL intensity plot is given in the inset.

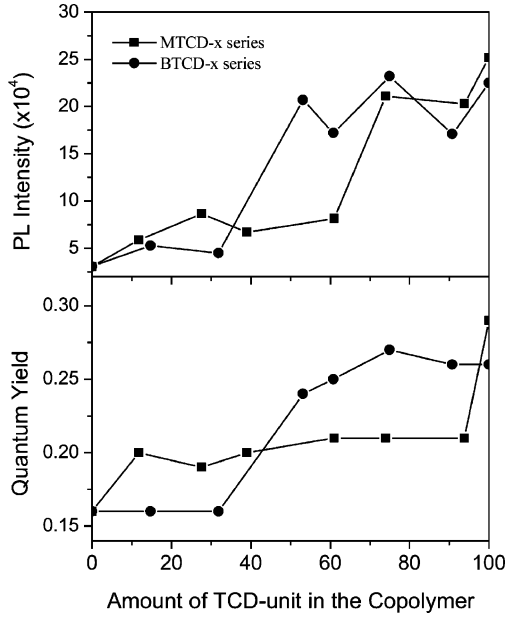

Figure 4. Plot of PL intensity and solution quantum yield of bulky PPV copolymers vs amount of TCD unit in the copolymer.

their solution quantum yields were plotted against their composition and are shown in Figure 4. The copolymers showed an interesting observation that the quantum yield of the copolymers increases with increase in their TCD content and

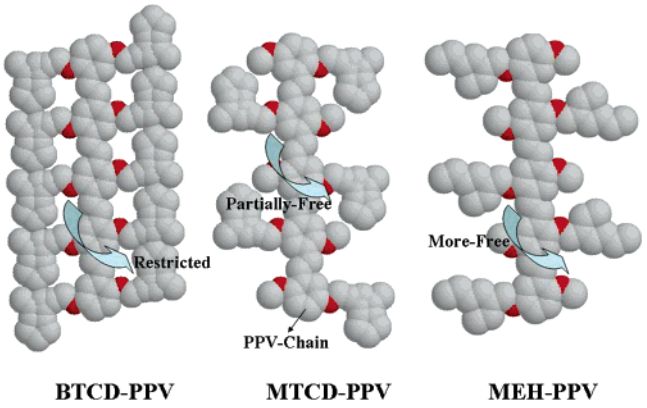

Figure 5. CPK space-filling models of the bulky PPV repeating units.

attained the values of their homopolymers. The PL properties of the copolymers also followed a similar trend as seen in the solution quantum yield. The enhancement in the PL intensity and quantum yield is more significant in the case of bis-TCD substitution compared to that of the mono-TCD. For example, the copolymers having more than 50% of BTCD units showed enhancement in luminescence intensities as equal to that of 75% MTCD units. The present investigation reveals that the presence of more than 50% of BTCD or 75% of MTCD−PPV in MEH−PPV increases the quantum yield by 2 and 4−5 times in PL intensity of PPV polymers.

CPK space-filling models of the BTCD−PPV, MTCD−PPV, and MEH−PPV polymer segments are shown in Figure 5. In general, the formation of aggregates in polymer matrix is induced by two factors: (i) the free volume available for chain folding and (ii) the existence of various secondary interactions such as π-stacking of conjugated systems as in the present case. The CPK model of the BTCD segment indicates that the symmetrically substituted TCD units enhance the steric hindrance, and very little space is available for interdigitization of the polymer chains and π-stack-induced molecular aggregation. The steric hindrance is also effective in the MTCD−PPV, but not to that extent compared to its bis-TCD counterpart. In the case of MEH−PPV, there is a substantial amount of free space available for the chain folding or interdigitization of the polymer chains. Since the aggregates are mainly driven by $\pi-\pi$ interactions, it is believed that the methoxy substituents are too short to provide adequate shielding of the backbone to avoid interbackbone contacts in MEH−PPV.[8] The model clearly

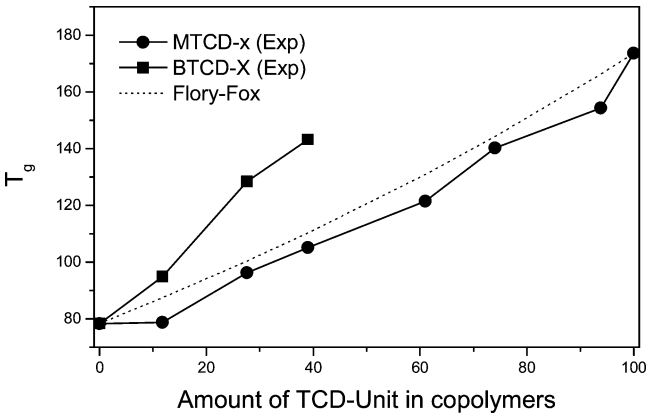

Figure 6. Plot of glass transition temperature (°C) vs amount of TCD unit in the copolymers.

demonstrates that the TCD unit is very rigid and capable of increasing the interchain distances in PPV. The increase in the interchain distance controls the molecular aggregation for significant enhancement in the solid-state photoluminescence. According to the CPK model (in Figure 5), one would anticipate that the rigidity of the BTCD−PPV should be high compared to MTCD and MEH backbone due to the little free space available for polymer chain folding. The glass transition temperature (T_g) of the polymer is a powerful tool to measure the rigidity of the polymer backbone. Highly rigid polymers are less susceptible for chain folding, and their T_g's are expected to be higher than that of the flexible ones. All the polymers were subjected to thermal analysis by DSC, and the DSC thermograms of polymers have shown only a glass transition (see Table 2), and no melting transitions or crystallization were observed (see Table 2). The T_g of MTCD−PPV is obtained as 174 °C, which is almost 100 °C higher than that of MEH−PPV (78 °C). The T_g's of the MTCD-*x* copolymers were plotted for various compositions and shown in Figure 6. Typically, random copolymers follow the Flory−Fox trend, and only those copolymers which have additional secondary interactions are expected to deviate from the equation. The Flory−Fox equation for the copolymer is

$$1/T_g = w_1/T_{g1} + w_2/T_{g2}$$

where w_1 and w_2 are the weight fractions and T_{g1}, T_{g2}, and T_g are glass transition temperatures of the homopolymers 1 and 2 and the copolymer, respectively.[56] The theoretical Flory−Fox plot for MTCD-*x* was plotted and shown along with the experimental data in Figure 6, and it is very clear from the plot that the MTCD-*x* follows exactly the Flory−Fox trend. It confirms that the repeating units are randomly distributed in the polymer chain. Though the π-stacking is known as a strong secondary interaction for molecular aggregation in conjugate polymers, its influence on the thermal transitions such as T_g is less significant. The glass transition temperature of the BTCD−PPV, BTCD-75, and BTCD-91 could not be determined by DSC techniques since they are highly amorphous, and Chou et al. have also reported similar difficulties in the determination of the T_g for highly rigid silsesquioxane substituted PPVs.[41] The BTCD-*x* copolymers also followed a linear trend (see Figure 6) with their compositions, which confirms that increasing the amount of bis-TCD-in the copolymer increases the rigidity of the PPV backbone as seen in the MTCD-*x* copolymer. It is very interesting to note that the BTCD-*x* copolymers have a much higher T_g compared to that of the MTCD-*x* copolymer. By extra-plotting the linear plot of the BTCD-*x* series, the T_g of the BTCD−PPV can be obtained as 200 °C, which is 25 and 125 °C higher than that of MTCD−PPV and MEH−PPV, respectively. The thermal analysis of copolymers confirmed that the introduction of the TCD unit increases the rigidity of the PPV backbone, and the increase is more in the case of bis-TCD, which supports the CPK space-filling model. Therefore, the increase in the PL intensity and quantum yield of the copolymer (in Figure 4) is mainly due to the increase in the rigidity of the polymer chains. The highly rigid polymer backbone restricts the chain folding (in the higher T_g polymers) and controls the molecular aggregation in the solid state for enhanced luminescent properties.

To trace the origin for the highly luminescent behavior of the bulky PPVs on a molecular level, we have synthesized three oligo(phenylenevinylene)s (OPVs) with methoxy, 2-ethylhexyloxy, and 1,8-tricyclodecanemethyeleneoxy groups in the middle aromatic rings. These OPVs are structurally identical to the MEH−PPV, MTCD−PPV, and BTCD−PPV polymer backbone. The absorbance and emission properties of these oligomers are summarized in Table 3. The absorbance and emission spectra of the model compounds in solid state are given in Figure 7. The absorbance spectra of the MTCD−OPV and BTCD−OPV were 2−5 nm blue-shifted compared to MEH−OPV, which indicates that the TCD substitution affects the planarity of the OPV similar to that of the PPV polymers. The solution quantum yields of the model compounds were determined using quinine sulfate as standard following a similar procedure described for the polymers. The model compounds have quantum yield in the range 0.50−0.54, which is normally reported for oligo(phenylenevinylene)s.[44,47] Recently, Carlos and Reddy and coworkers[51,53] have reported that solid-state luminescent quantum yield of the organic or organic−inorganic emitters can be determined for powdered samples following the equation described by Brill et al.:[50]

$$\phi = \phi_s(1 - r_s/1 - r_x)(A_x/A_s)$$

where r_s and r_x are the diffuse reflectance (with respect to a fixed wavelength) of the standard and sample, respectively, and ϕ_s is the quantum yield of the standard phosphor. The terms A_x and A_s represents the area under the peaks of the sample and the standard emission spectra, respectively. Diffused reflectance and emission spectra were acquired by following the reported procedure, and in order to have absolute intensity values $BaSO_4$ was used as reflecting standard (r = 91%). To prevent insufficient absorption of the exciting radiation, a fine powder sample of the model compounds was loaded as uniform layer of 3 mm thickness in the sample holder to ensure that only the sample was illuminated, in order to diminish the quantity of light scattered by the front sample holder. Dry sodium salicylate was used as reference whose emission spectra are formed by a large broad band peaking around 425 nm, with a constant ϕ value (60%) for excitation wavelengths between 220 and 380 nm. The excitation spectra of the model compounds and the standard indicate that samples have overlap with the standard in the region of 310−370 nm, and therefore, the above approach can be directly utilized to determine the solid-state quantum yield. The quantum yields of the model compounds were determined using various excitation wavelengths in the 310−370 nm region, and the values are shown as the inset in Figure 7. It is very clear from the plots that the absolute solid-state quantum yields of the compounds are almost the same for various excitation wavelengths, and the values were obtained with ±10% experimental limit as reported by others.[53] The quantum yields of the MEH−OPV, MTCD−OPV, and BTCD−

Table 3. Photophysical and Thermal Properties of the Bulky OPV Compounds

sample	λ_{max} (in $CHCl_3$) (abs)	λ_{max}[a] (in $CHCl_3$) (em)	ϕ_{FL}[b] (in $CHCl_3$)	λ_{max}(film) (abs)	λ_{max}(powder) (em)	ϕ_{PL}[c]	T_D[d] (°C)	T_m[e] (°C)
MEH−OPV	324, 389	433, 469	0.53	387	525	0.27	298	54
MTCD−OPV	324, 386	431, 468	0.50	385	499	0.82	285	176[e]
BTCD−OPV	324, 386	432, 471	0.54	382	525	0.64	343	226[e]

[a] Absorption and emission studies were done in chloroform, and the excitation wavelength used is 380 nm for all the compounds. [b] Calculated using quinine sulfate as standard and excited at 380 nm; the absorbance of solutions was maintained as 0.1 at 380 nm. [c] Absolute solid-state quantum yields were determined by the diffuse reflectance method using sodium salicylate as standard. [d] Decomposition temperature at 10% weight loss. [e] Melting temperature was obtained from DSC analysis at 10 °C/min heating rate, and other values corresponding to nematic LC phases are given in Figure 8.

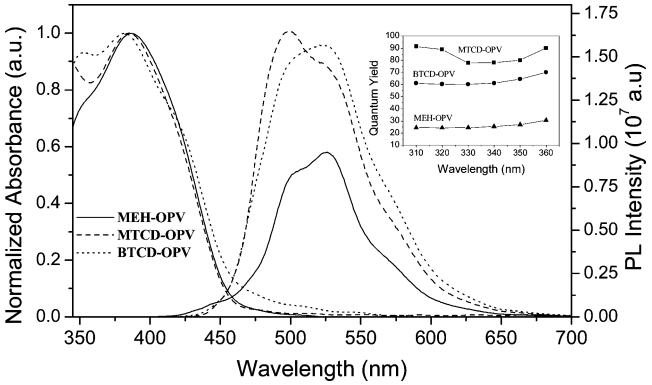

Figure 7. Solid-state absorption and emission spectra of OPVs. The plot of excitation wavelength vs quantum yield (%) is given in the inset.

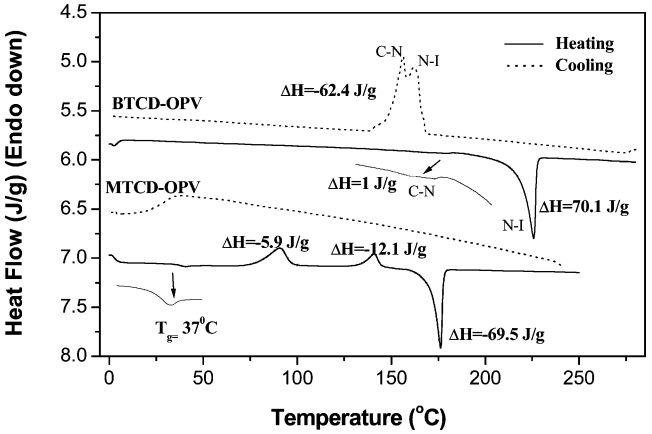

Figure 8. DSC thermograms of the BTCD−OPV and MTCD−OPV.

OPV were calculated by taking the average values for the excitation in the region 330−360 nm (flat region) and reported in Table 3. It is very interesting to note that the bulky TCD model compounds BTCD−OPV and MTCD−OPV have quantum yields of 0.64 and 0.82, respectively, which is 2−3 times higher than that of MEH−OPV ($\phi = 0.27$). It clearly demonstrates that the bulky TCD unit is very efficient structure directing unit for highly luminescent π-conjugated materials. Surprisingly, the mono-TCD substitution enhances the solid-state luminescence in the OPV backbone much higher than that of the bis-TCD. It may be due to the difference in the three-dimensional arrangement or packing of the molecules in MTCD−OPV and BTCD−OPV.

The three-dimensional solid-state packing of small molecules can be understood from the crystallization and melting behaviors, and therefore, the OPVs were subjected to thermal analysis by DSC. The DSC thermograms of the model compounds are shown in Figure 8. MEH−OPV showed a melting transition in the first heating cycle; however, it failed to show any peaks in the subsequent heating/cooling cycles (see Supporting Information). Interestingly, BTCD−OPV showed liquid crystalline (LC) behavior while cooling from the melt, and two crystallization exotherms at 162 and 156 °C were observed, corresponding to their isotropic-to-LC and LC-to-crystalline. In the subsequent heating cycle, it showed weak transition at 176 °C for crystalline-to-LC and the LC-to-isotropic at 226 °C. The thermal properties of MTCD−OPV were observed completely different, and it did not show any crystallization peak while cooling from melt; only a broad glass transition is observed below 40 °C. In the subsequent heating cycle, the glass transition is reappeared again at 37 °C (see inset), and two residual cooled crystallization peaks appeared at 90 and 141 °C, which are completely melted at 176 °C. Attempts were also made to crystallize the MTCD−OPV at much lower cooling rates such as 5 to 1 °C/min, but only a glass transition was observed. It indicates that the crystallization process of MTCD−OPV is completely different from BTCD−OPV, and the former has less of a tendency to crystallize compared to the highly ordered liquid crystalline BTCD−OPV. In general, while cooling from melt, semicrystalline polymeric (or oligomeric) materials tend to organize in highly ordered crystalline state or disordered amorphous domains.[44,57] The extent to which the materials crystallize out or frozen into an amorphous domain is highly dependent upon their structure of the backbone. The enthalpies of melting endotherms for both MTCD−OPV (69.5 J/g) and BTCD−OPV (70.1 J/g) are almost comparable, which indicate that both molecules originally possess the same amount of percent crystallinity. The enthalpy of crystallization exotherm in BTCD−OPV (62.4 J/g) is almost 90% of its heating endotherm (70.1 J/g), which indicates that most of the materials are crystallized out in the liquid crystalline phases in cooling cycle. In the case of MTCD−OPV, no crystallization occurred from the melt, and almost all the materials are trapped into amorphous domains. In the subsequent heating cycle, above the glass transition, the trapped molecules in amorphous domain undergo ordering and produce residual cooling crystallization exotherms, which is only 25% (5.9 + 12.1 J/g) of its entire heating endotherm (69.5 J/g). It reveals that in MTCD−OPV more than 75% of the materials are frozen while cooling from the melt in the amorphous domains, which contributes the large glass transition at 37 °C. Introduction of liquid crystallinity in the poly(phenylenevinylene)s were reported using diethylhexyl,[58] oxadiazole,[59] dimethyloctylsilyl,[60] biphenyl,[61] cyanobiphenyl,[62] cyclohexylphenyl,[63] trialkoxygallic, and dendritic[29] units as pendants in the PPV backbone. Almost all these LC−PPVs showed a nematic texture, and the LC transition temperature was observed in the range 170−200 °C. Maddux et al. reported an orthogonal approach for developing LC oligo(phenylenevinylene)s (OPVs), and they have reported that the LC transition increases (from 85 to 185 °C) with increase in the oligomers length from 4 to 12.[47] Strehmel et al. had reported LC−OPVs containing octyl or fluoro substitution, and these LC−OPV molecules were found to have much lower LC transition (60−80 °C).[64] Interestingly, the bis-TCD substituted oligomer (BTCD−OPV) studied here showed a thermotropic LC behavior, whereas its polymer

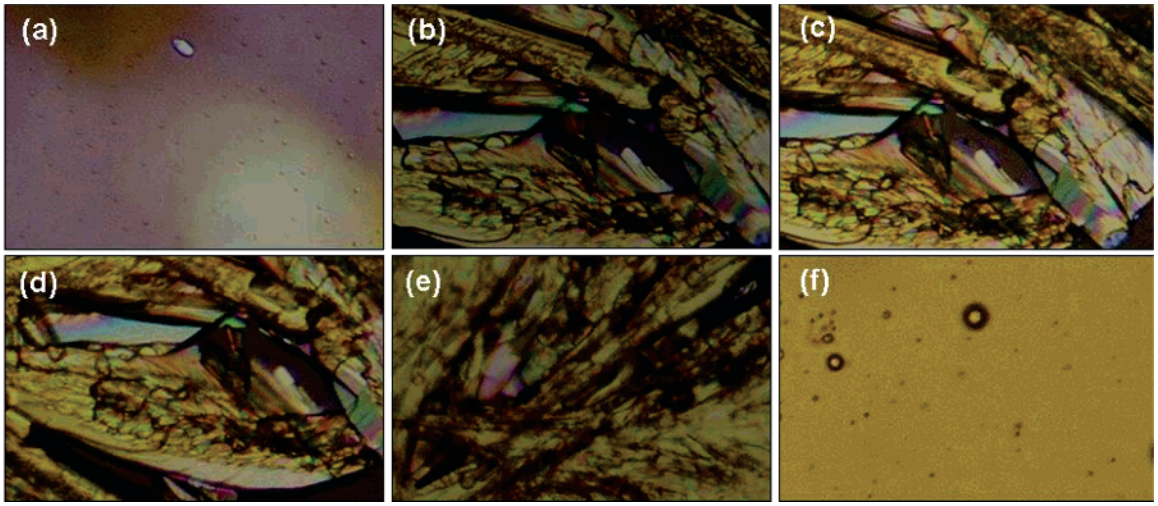

Figure 9. Polarizing light microscopic photographs of BTCD−OPV at 260 °C (isotropic) (a), while cooling from isotropic at 10 °C/min [164 (b) and 144 °C (c)] and in the second heating at 10 °C/min [93 (d), 162 (e), and 230 °C (f) (isotropic)].

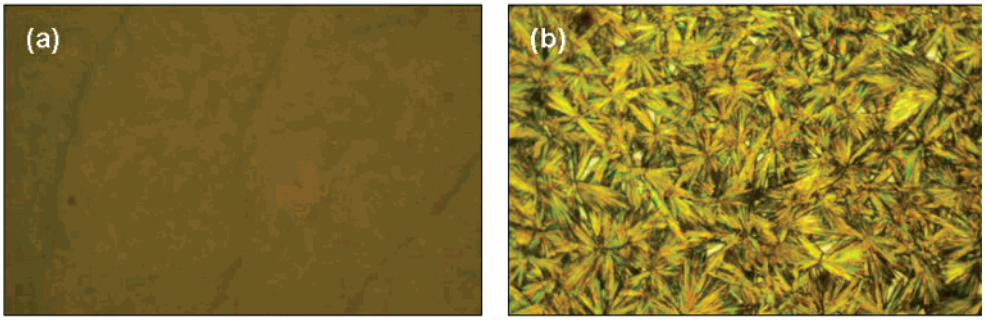

Figure 10. Polarizing light microscopic photographs of MTCD−OPV in the cooling cycle from isotropic at 10 °C/min [230 to 30 °C (a) same amorphous nature] and in the second heating at 10 °C/min [at 140 °C (b), residual crystallized materials from glassy state].

(BTCD−PPV) did not show any LC behavior and only T_g was observed. The LC transition temperature of the BTCD−OPV was found as 170−200 °C, which is much higher compared to the octyl-substituted OPV reported earlier.[47,64] It indicates that the bulky TCD unit is highly rigid pendant group, and its substitution in OPVs can increase the LC transition temperature to the level of LC-PPVs. Additionally, the liquid crystalline alignment of BTCD−OPV enhances the solid-state photoluminescence quantum yield, which is rarely noticed for other types of pendants indicated above in either OPVs or PPVs.

In order to confirm the LC behavior of the BTCD−OPV, it was subjected to polarizing light microscopic (PLM) analysis using a temperature-controlled hot stage. The sample was heated to melt at 10 °C/min and isothermally maintained for 3 min (melt appeared dark under the polarizer and no crystallites were visible), and the melt was subsequently control cooled at 10 °C/min. The liquid crystalline phases of the BTCD−OPV at various temperatures are shown in the photographs in Figure 9. BTCD−OPV was completely melted at 260 °C, and it was held at this temperature for 2 min (Figure 9a). While cooling from the melt, the LC phases started to appear initially as small nucleation sites which then flowed and started to form a uniform threadlike pattern corresponding to nematic LC phases (at 164 °C (Figure 9b)). On further cooling, the texture was found to remain the same (at 144 °C (Figure 9c)) and unaltered up to room temperature, which suggests that the LC phases can be frozen in the polymer matrix. In the subsequent heating (at 10 °C/min), the LC phases remain the same [at 93 °C (Figure 9d) and 162 °C (Figure 9e)] and disappeared at high temperature (at 230 °C, Figure 9f). It is very clear from the photographs in Figure 9 that all the BTCD−OPV showed a clear nematic LC phase, and the phase transitions are in accordance with their DSC thermograms. On the other hand, up on cooling from the melt (see Figure 10), the MTCD−OPV remains isotropic (or glassy) up to room temperature (Figure 10a). In the subsequent heating cycle, the residual crystallization starts at 80 °C, and nice spherulitic crystals were noticed at 140 °C (Figure 10b), which melted at the high temperature. It suggests that MTCD−OPV molecules have a tendency to form less crystalline and glassier materials while cooling, and it may be associated with its unsymmetrical substitution in the backbone. It indicates that the mono-TCD substitution in the OPV backbone hinders the perfect packing of the molecules in the solid state, which in turn forces the entire matrix to trap in the amorphous domain. In the case of BTCD−OPV, the symmetric structure enhances the parallel arrangements of the molecules and leads to thermoreversible nematic liquid crystalline material. Our preliminary attempts to study the single-crystal structure for the model compounds were not successful, and the work is currently in progress to support the packing of the chromophores. Nevertheless, the DSC and PLM studies reveal that the enhancement of solid-state quantum yield in MTCD−OPV by almost 1.3 times compared to BTCD−OPV is a result of the amorphous nature of the former compared to that of the ordered liquid crystalline BTCD−OPV. BTCD−OPV is a new and promising luminescent emitter with 64% solid-state quantum yield for liquid crystalline display systems. MTCD−OPV is another interesting glassy emitter for optoelectronic devices, which is the first oligo(phenylenevinylene) in the literature with more thane 82% solid-state luminescent quantum yield. In the present study, we have successfully demonstrated that the chemical structure of the bulky-π-conjugated materials play a

major role in the manipulation of solid-state luminescent intensity, quantum yield, liquid crystalline and amorphous glassy nature of poly(phenylenevinylene)s and its triad oligomers.

Conclusion

In conclusion, we have demonstrated that the tricyclodecane bulky group is an efficient structure directing pendant for highly luminescence π-conjugated materials, more specifically PPVs and OPVs. The solid-state luminescence can be enhanced by 4−5 times compared to that of MEH−PPV by the TCD substitution, and it was shown that the chemical structure of the polymer plays a major role in the photoluminescence enhancement. Two series of bulky PPV copolymers (MTCD-*x* and BTCD-*x*) were prepared by varying the entire compositing range from 0 to 100%, and the NMR signals of the structurally similar OPVs were utilized to determine the compositions. The compositions vs glass transitions of the copolymers followed the Flory−Fox trend, and the T_g of the copolymers linearly increases with the compositions. The increasing trend of T_g indicates the increase in the rigidity in the copolymers with TCD substitution, and the highly rigid structure has less tendency for molecular aggregation as supported by the CPK space-filling model. The increasing rigidity in the PPV backbone minimizes the aggregation, and the copolymers with higher TCD content possess enhanced PL intensity and solution quantum yield. MTCD-*x* and BTCD-*x* copolymers were highly soluble (like MEH−PPV) with high photoluminescence efficiency and may have great potential as various optoelectronic materials. Diffuse reflectance measurements were performed on the structurally similar OPVs, and their high absolute solid-state quantum yield supports the high PL intensity of the bulky PPVs. Nematic liquid crystalline or amorphous glassy OPVs were easily obtained by bis- or mono-TCD substitution in the oligomers, which have great potential as bright luminescence materials. We are currently in the process of studying the device performance of these new polymers and oligomers in collaboration with expert research group, which will be published elsewhere.

Acknowledgment. We thank KSCTSE, Thiruvananthapuram, Kerala, India (082/SRSPS/2004/CSTE), and CSIR-task force (COR-0004), New Delhi, India, for financial support. S. R. Amrutha thanks CSIR-New Delhi, India, for a research fellowship. We greatly acknowledge Celanese Chemicals Ltd. for providing TCD research samples. We also thank Dr. Suresh das, RRL-Trivandrum, for the PLM facilities.

Supporting Information Available: Copolymer composition determination by ^{1}H NMR and FT-IR spectra, elemental analysis data, solution state emission spectra of polymers, solid-state excitation spectra of polymers, DSC thermogram of MEH−OPV, and size exclusion chromatogram and HR-FAB mass spectra of OPVs. This material is available free of charge via the Internet at http://pubs.acs.org.

References and Notes

(1) Burroughes, J. H.; Bradley, D. D. C.; Brown, A. R.; Marks, R. N.; Mackay, K.; Friend, R. H.; Burns, P. L.; Holmes, A. B. *Nature (London)* **1990**, *347*, 539.
(2) Friend, R. H.; Gymer, R. W.; Holmes, A. B.; Burrouges, J. H.; Marks, R. N.; Taliani, C.; Bradley, D. D. C.; dos Santos, D. A.; Gredas, J. L.; Longlund, M.; Salaneck, W. R. *Nature (London)* **1999**, *397*, 121.
(3) Sheats, J. R.; Antoniadis, H.; Hueschen, M.; Leonard, W.; Miller, J.; Moon, R.; Roitman, D.; Stocking, A. *Science* **1996**, *273*, 884.
(4) Kraft, A.; Grimsdale, A. C.; Holmes, A. B. *Angew. Chem., Int. End. Engl.* **1998**, *37*, 402.
(5) Lidzey, D. G.; Bradley, D. D. C.; Alvarado, S. F.; Seidler, P. F. *Nature (London)* **1997**, *386*, 135.
(6) Akcelrud, L. *Prog. Polym. Sci.* **2003**, *28*, 875.
(7) Kim, J. *Pure Appl. Chem.* **2002**, *74*, 2031.
(8) (a) Jenekhe, S. A.; Osaheni, J. A. *Science* **1994**, *265*, 765. (b) Huang, W. Y.; Matsuoka, S.; Kwei, T. K.; Okamoto, Y. *Macromolecules* **2001**, *34*, 7166. (c) Chen, S. H.; Su, A. C.; Han, S. R.; Chen, S. A.; Lee, Y. Z. *Macromolecules* **2004**, *37*, 181. (d) Breitenkamp, R. B.; Tew, G. N. *Macromolecules* **2004**, *37*, 1163. (e) Wang, P.; Collison, C. J.; Rothberg, L. J. *J. Photochem. Photobiol. A: Chem.* **2001**, *144*, 63. (f) Peng, K. Y.; Chen, S. A.; Fann, W. S.; Chen, S. H.; Su, A. C. *J. Phys. Chem. B* **2005**, *109*, 9368.
(9) Collison, C. J.; Rothberg, L. J.; Treemaneekarn, V.; Li, Y. *Macromolecules* **2001**, *34*, 2346.
(10) Shi, Y.; Liu, J.; Yang, Y. *J. Appl. Phys.* **2000**, *87*, 4254.
(11) Jakubiak, R.; Collison, C. J.; Wan, W. C.; Rothberg, L. J.; Hsieh, B. R. *J. Phys. Chem. A* **1999**, *103*, 2394.
(12) Marchioni, F.; Chiechi, R.; Patil, S.; Wudl, F.; Chen, Y.; Shinar, J. *Appl. Phys. Lett.* **2006**, *89*, 61101.
(13) Nguyen, T. Q.; Doan, V.; Schwartz, B. J. *J. Chem. Phys.* **1999**, *110*, 4068.
(14) Chou, H. L.; Lin, K. F.; Fan, Y. L.; Wang, D. C. *J. Polym. Sci., Polym. Phys.* **2005**, *43*, 1705.
(15) Padmanabhan, G.; Ramakrishnan, S. *J. Am. Chem. Soc.* **2000**, *122*, 2244.
(16) Liao, L.; Pang, Y.; Ding, L.; Karasz, F. E.; Smith, P. R.; Meador, M. A. *J. Polym. Sci., Polym. Chem.* **2004**, *42*, 5853.
(17) (a) Liao, L.; Pang, Y.; Ding, L.; Karasz, F. E. *Macromolecules* **2002**, *35*, 3819. (b) Pang, Y.; Li, J.; Hu, B.; Karasz, F. E. *Macromolecules* **1999,** *32*, 3946.
(18) Liao, L.; Pang, Y.; Ding, L.; Karasz, F. E. *Macromolecules* **2001**, *34*, 6756.
(19) Zheng, M.; Sarker, A. M.; Gurel, E. E.; Lahti, P. M.; Karaz, F. E. *Macromolecules* **2000**, *33*, 7426.
(20) (a) Chu, Q.; Pang, Y. *Macromolecules* **2003**, *36*, 4614. (b) Chu, Q.; Pang, Y. *Macromolecules* **2005**, *38*, 517.
(21) Haung, C.; Haung, W.; Guo, J.; Yang, C. Z.; Kang, E. T. *Polymer* **2001**, *42*, 3929.
(22) Li, K.; Wang, Q. *Macromolecules* **2004**, *37*, 1172.
(23) Cho, H.; Kim, E. *Macromolecules* **2002**, *35*, 8684.
(24) Li, W.; Wang, H.; Yu, L.; Morkved, T. L.; Jaeger, H. M. *Macromolecules* **1999**, *32*, 3034.
(25) (a) Chou, C. H.; Hsu, S. L.; Dinakaran, K.; Chiu, M. Y.; Wei, K. H. *Macromolecules* **2005**, *38*, 745. (b) Xia, C.; Advincula, R. C. *Macromolecules* **2001**, *34*, 5854.
(26) (a) Yang, J. S.; Swager, T. M. *J. Am. Chem. Soc.* **1998**, *120*, 5321. (b) Yang, J. S.; Swager, T. M. *J. Am. Chem. Soc.* **1998**, *120*, 11864.
(27) Wang, H.; Song, N.; Li, H.; Li, Y.; Li, X. *Synth. Met.* **2005**, *151*, 279.
(28) Tang, R.; Chuai, Y.; Cheng, C.; Xi, F.; Zou, D. *J. Polym. Sci., Polym Chem.* **2005**, *43*, 3126.
(29) Bao, Z.; Amundson, K. R.; Lovinger, A. J. *Macromolecules* **1998**, *31*, 8647.
(30) Ko, S. W.; Jung, B. J.; Cho, N. S.; Shim, H. K. *Bull. Korean Chem. Soc.* **2002**, *23*, 1235.
(31) Choo, D. J.; Talaie, A.; Lee, Y. K.; Jang, J.; Park, S. H.; Huh, G.; Yoo, K. H.; Lee, J. Y. *Thin Solid Films* **2000**, *363*, 37.
(32) Ahn, T.; Ko, S. W.; Shim, H. K. *Macromolecules* **2002**, *35*, 3495.
(33) Jeong, H. Y.; Lee, Y. K.; Talaie, A.; Kim, K. M.; Kwon, Y. D.; Jang, Y. R.; Yoo, K. H.; Choo, D. J.; Jang, J. *Thin Solid Films* **2002**, *417*, 171.
(34) Lee, Y. K.; Jeong, H. Y.; Kim, K. M.; Kim, J. C.; Choi, H. Y.; Kwon, Y. D.; Choo, D. J.; Jang, Y. R.; Yoo, K. H.; Jang, J.; Talaie, A. *Curr. Appl. Phys.* **2002**, *2*, 241.
(35) Anderson, M. R.; Yu, G.; Heeger, A. J. *Synth. Met.* **1997**, *85*, 1275.
(36) Wudl, F.; Hoger, S.; Zhang, C.; Pakbaz, K.; Heeger, A. J. *Polym. Prepr.* **1993**, *34*, 197.
(37) (a) Mikroyannidis, J. A. *Macromolecules* **2002**, *35*, 9289. (b) Spiliopoulos, I. K.; Mikroyannidis, J. A. *Macromolecules* **2002**, *35*, 2149. (c) Spreitzer, H.; Becker, H.; Kluge, E.; Kreuder, W.; Schenk, H.; Demandt, R.; Schoo, H. *Adv. Mater.* **1998**, *10*, 1340. (d) Johansson, D. M.; Srdanov, G.; Yu, G.; Theander, M.; Inganas, O.; Andersson, M. R. *Macromolecules* **2000**, *33*, 2525. (e) Hsieh, B. R.; Yu, Y.; Forsythe, E. W.; Schaaf, G. M.; Feld, W. A. *J. Am. Chem. Soc.* **1998**, *120*, 231. (f) Wan, W. C.; Antoniadis, H.; Choong, V. E.; Razafitrimo, H.; Gao, Y.; Feld, W. A.; Hseih, B. R. *Macromolecules* **1997**, *30*, 6567. (g) Lee, S. H.; Jang, B. B.; Tsutsui, T. *Macromolecules* **2002**, *35*, 1356. (h) Chen, Z. K.; Lee, N. H. S.; Huang, W.; Xu, Y. S.; Cao, Y. *Macromolecules* **2003**, *36*, 1009.
(38) Sarker, A. M.; Ding, L.; Lahti, P. M.; Karasz, F. E. *Macromolecules* **2002**, *35*, 223.
(39) Lee, N. H. S.; Chen, Z. K.; Huang, W.; Xu, Y. S.; Cao, Y. *J. Polym. Sci., Polym. Chem.* **2004**, *42*, 1647.

(40) Chen, Z. K.; Wang, L. H.; Kang, E. T.; Huang, W. *Phys. Chem. Chem. Phys.* **1999**, *1*, 3789.
(41) Chou, C. H.; Hsu, S. L.; Yeh, S. W.; Wang, H. S.; Wei, K. H. *Macromolecules* **2005**, *38*, 9117.
(42) Xiao, S.; Nguyen, M.; Gong, X.; Cao, Y.; Wu, H.; Moses, D.; Heeger, A. J. *Adv. Funct. Mater.* **2003**, *13*, 25.
(43) Tokito, S.; Tanaka, H.; Noda, K.; Okada, A.; Taga, Y. *Appl. Phys. Lett.* **1997**, *70*, 1929.
(44) He, F.; Xu, H.; Yang, B.; Duan, Y.; Tian, L.; Huang, K.; Ma, Y.; Liu, S.; Feng, S.; Shen, J. *Adv. Mater.* **2005**, *17*, 2710.
(45) Oelkrug, D.; Tompert, A.; Gierschner, J.; Egelhaaf, H. J.; Hanack, M.; Hohloch, M.; Steinhuber, E. *J. Phys. Chem. B* **1998**, *102*, 1902.
(46) Jin, J.; Smith, D. W., Jr.; Glasser, S.; Perahia, D.; Foulger, S. H.; Ballato, J.; Kang, S. W.; Kumar, S. *Macromolecules* **2006**, *39*, 4646.
(47) Maddux, T.; Li, W.; Yu, L. *J. Am. Chem. Soc.* **1997**, *119*, 844.
(48) Amrutha, S. R.; Jayakannan, M. *J. Phys. Chem. B* **2006**, *110*, 4083.
(49) Jancy, B.; Asha, S. K. *J. Phys. Chem. B* **2006**, *110*, 20937.
(50) Bril, A.; De Jager-Veenis, A. W. *J. Electrochem. Soc.* **1976**, *123*, 396.
(51) Biju, S.; AmbiliRaj, D. B.; Reddy, M. L. P.; Kariuki, B. M. *Inorg. Chem.* **2006**, *45*, 10651.
(52) eSilva, F. R. G.; Menezes, J. F. S.; Rocha, G. B.; Alves, S.; Brito, H. F.; Longo, R. L.; Malta, O. L. *J. Alloys Compd.* **2000**, *364*, 303−304.
(53) Fu, L.; Ferreira, R. A. S.; Silva, N. J. O.; Fernandes, A. J.; Ribeiro-Claro, P.; Goncalves, I. S.; Bermudez, V. Z.; Carlos, L. D. *J. Mater. Chem.* **2005**, *15*, 3117.
(54) Fan, Q. L.; Lu, S.; Lai, Y. H.; Hou, X. Y.; Huang, W. *Macromolecules* **2003**, *36*, 6976.
(55) Egbe, D. A. M.; Tillmann, H.; Rirckner, E.; Klemm, E. *Macromol. Chem. Phys.* **2001**, *202*, 2712.
(56) (a) Deepa, P.; Divya, K.; Jayakannan, M. *J. Polym. Sci., Polym. Chem.* **2006**, *44*, 42. (b) Deepa, P.; Sona, C.; Jayakannan, M. *J. Polym. Sci., Polym. Chem.* **2006**, *44*, 5557.
(57) Jayakannan, M.; Ramakrishnan, S. *J. Polym. Sci., Polym. Chem.* **1998**, *36*, 309.
(58) Olsen, B. D.; Jang, S. Y.; Luning, J. M.; Segalman, R. A. *Macromolecules* **2006**, *36*, 4469.
(59) Sun, X.; Li, M.; Liu, D.; Zhang, P.; Tian, W. *J. Appl. Polym. Sci.* **2004**, *91*, 396.
(60) Hwang, D. H.; Shim, H. K. *Thin Solid Films* **2002**, *417*, 166.
(61) Li, A. K.; Yang, S. S.; Jean, W. Y.; Hsu, C. S. *Chem. Mater.* **2000**, *12*, 2741.
(62) Akagi, K.; Oguma, J.; Shibata, S.; Toyoshima, R.; Osaka, I.; Shirakawa, H. *Synth. Met.* **1999**, *102*, 1287.
(63) Oguma, J.; Akagi, K.; Shirakawa, H. *Synth. Met.* **1999**, *101*, 86.
(64) Strehmel, B.; Sarker, A. M.; Malpert, J. H.; Strehmael, V.; Seifert, H.; Neckers, D. C. *J. Am. Chem. Soc.* **1999**, *121*, 1226.

MA062764Q